

Microstructural evolution of bulk nanocrystalline Ni during creep

Manish Chauhan · Farghalli A. Mohamed

Received: 2 June 2006 / Accepted: 18 August 2006 / Published online: 4 January 2007
© Springer Science+Business Media, LLC 2006

Abstract Experiments were conducted on electrodeposited (ED) nanocrystalline (nc) Ni with an average initial grain size of about 20 nm at 393 K to study the shape of the creep curves. In addition, microstructure was examined by means of transmission electron microscopy (TEM). The results show that the creep curves are characterized by the presence of a well-defined steady-state stage. An examination of the microstructure indicates that while grain growth occurs during deformation, the grain size attains a constant value once steady state creep is approached. A comparison between grain size measurements obtained by the TEM technique and those obtained via the X-ray diffraction method shows that the use of the latter method may lead to an underestimation of the value of the average grain size.

Introduction

Nanocrystalline (Nc) materials are defined, in general, as polycrystalline materials with grain sizes in the range of 1–100 nm in at least one dimension. Because of their extremely fine grain size, there is a significant increase in the volume fraction of grain boundaries, junction lines and nodal points that may influence properties far more strongly than in more conventional microstructures [1–3]. Nc-materials have novel physical, chemical,

biological and mechanical properties that may have important engineering applications. As a consequence, they are attracting wide attention in materials research.

In this paper, experimental data obtained in an investigation on deformation behavior and microstructure in bulk nc-Ni prepared by an electrodeposition (ED) technique are reported and analyzed. The investigation was motivated by two primary considerations.

First, it is well documented that when large-grained metals, such as Ni, are crept under the conditions of constant temperature and constant stress, the creep curve, which represents the plot of strain against time, is characterized by a secondary stage in which the creep rate remains constant [4]. This stage is referred to as the steady state stage, and its presence reflects the presence of a balance between strain hardening and recovery. By contrast, evidence regarding the existence of steady-state creep in the creep curve of nc-metals is not well established. A case in point is the creep behavior of nc-Ni. On the one hand, the creep curves reported by Yin et al. [5] appeared to show that the creep rates were approaching steady state creep after 3% strain at 473 K and 200 MPa. On the other hand, the creep curves reported by Kottada and Chokshi [6] exhibited creep rates that decreased continuously with time. Furthermore, in most cases, creep strains associated with the creep curves reported for nc-metals do not exceed 0.01 [3, 5, 7–12]. With such small strains, it is not possible to ascertain the presence of steady state creep. Clarification of the above issue is essential for the full characterization of the creep behavior of nc-materials in terms of deformation mechanisms.

Second, grain size measurements in nc-metals have been performed using either X-ray diffraction (XRD)

M. Chauhan · F. A. Mohamed (✉)
Department of Chemical Engineering and Materials
Science, University of California, Irvine, CA 92697, USA
e-mail: famohame@uci.edu

or transmission electron microscopy (TEM) or both. In some cases, a comparison was made between the average initial grain sizes obtained by XRD and those measured by means of TEM. However, no detailed study has yet been attempted to compare grain sizes measured by both methods after deformation above room temperature, where grain growth may be significant. Such a study can provide information not only on the stability of grain size during deformation but also on the reliability of XRD in providing accurate measurements for grain size.

It is the purpose of this paper to report and analyze the data obtained in the present investigation.

Experimental procedure

Material and processing

(ED) nc-Ni was provided by Integran Technologies Inc., Toronto, Canada in the form of sheets with a thickness of 0.5 mm with an average initial grain size of 20 nm. (ED) nc-Ni was chosen for three primary reasons. First, (ED) nc-Ni has served as a model nc-material to investigate deformation and microstructure [5, 6, 10, 12–17]. Second, a direct comparison can be made between the results obtained in the present investigation above room temperature and those already available in the literature at room temperature. Third, according to available information [18] the ED route can produce a fully dense nc-Ni with a fairly narrow grain size distribution. These two advantages are critical in terms of investigating deformation mechanism.

The chemical composition of as-(ED) nc-Ni is given in Table 1. Chemical analysis shows the presence of small amount of impurities such as S and C.

Mechanical testing

The ED sheets of 0.5 mm thickness were machined to produce flat double-shear specimens [19, 20] whose gauge dimensions were: 0.5 mm (thickness) \times 2.5 mm (length) \times 2.5 mm (height) for creep testing.

Table 1 Chemical composition of as-electrodeposited nc-Ni

Elements	Wt. %
S	0.058
C	0.013
P	0.003
Si	<0.001
Cu	0.023
Co	0.071
Ni	Balance

Creep tests were conducted on a testing machine operated at constant load in a silicone oil bath at 393 K and 65 MPa to examine whether the creep curves exhibit a steady-state stage.

Three comments regarding the above experimental procedure and experimental conditions are in order. First, in performing creep tests, the double shear technique was utilized. Three factors favor testing double shear specimens over testing tensile specimens [21, 22]: (a) the problem of plastic instability (necking) that characterizes deformation under tension can be avoided, (b) strains produced by shear stresses, unlike those produced by tensile stresses, are not only uniform but also large, and (c) the procedure of testing is simplified since constant load implies constant stress on a creep machine. Second, the use of a silicone oil bath provides several advantages over that of a controlled-environment furnace in terms of (a) suitability for low-temperature testing, and (b) uniformity and stability of test temperature (to within ± 1 K) over a long period of time. The test temperature was monitored with chromel–alumel thermocouple held in contact with the specimen, and maintained to within ± 1 K of the reported temperature. Finally, the test temperature of 393 K was selected because recent results on (ED) nc-Ni have shown [14, 17] that upon annealing at temperatures < 473 K, sulfur segregation to boundaries are insignificant.

Prior to the application of the external load, specimens were left in the silicone oil bath after heating to the test temperature for 30 min to ensure that the temperature was stable. Creep tests were run for sufficiently large strains (> 0.06) to examine whether steady state creep existed. Strain was measured with a linear variable differential transducer (LVDT), equipped with an amplifier and was recorded using a computer-controlled data acquisition system. After the specimens had been strained under steady-state conditions, they were air-cooled rapidly under load to preserve the substructure.

Characterization

XRD measurements were conducted using a Siemens D5000 diffractometer equipped with a graphite monochromator using copper K_{α} ($\lambda = 0.15406$ nm) radiations. General scans with a step size of 0.01° (2θ) and with a step time of 2 s were conducted for grain size determination. Following subtraction of the instrumental broadening and $K_{\alpha 2}$ components, integral breadth for five strong FCC Ni peaks ($\{111\}$, $\{200\}$, $\{220\}$, $\{311\}$, and $\{222\}$) was measured.

A detailed TEM investigation on Ni samples (as-ED and deformed) was conducted using a Philips CM 20 TEM at 200 kV. The TEM sample preparation is similar to that reported elsewhere [23]. TEM thin foils were prepared for observation both in the plane and in the cross-section of the sample.

Experimental results

Uninterrupted and stress increase tests

Nc-Ni samples creep tested at 65 MPa and 393 K. Figure 1, in which shear strain is plotted as a function of time, shows a typical creep curve for (ED) nc-Ni at 65 MPa. An examination of the creep curve shows the presence of: (a) a primary creep stage that is fast in duration, and (b) a secondary stage that is well-defined.

In addition, specimens were crept and then the initial stresses were abruptly increased. An example for the results of stress increase tests is given in Fig. 2. Consideration of Fig. 2 demonstrates that steady-state creep rates are essentially reproducible, regardless of whether the creep rate was obtained from uninterrupted tested or stress increase tests.

Texture

Figure 3a provides a typical example for the XRD pattern of as-received nc-Ni. The XRD pattern shows strong orientation around (111) followed by (200), indicating a preference for the planes with the lowest

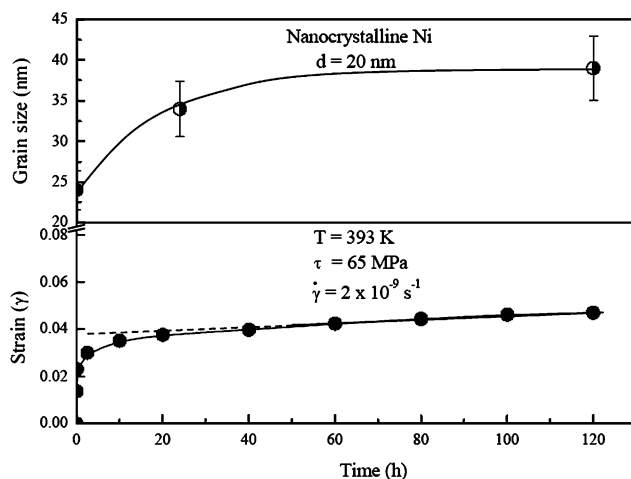


Fig. 1 A typical creep curve for (ED) nc-Ni (initial grain size = 20 nm) plotted as shear strain (γ) versus time at 65 MPa and 393 K (*lower portion*). Figure also shows the variation in the average grain size as a function of time during creep (*upper portion*)

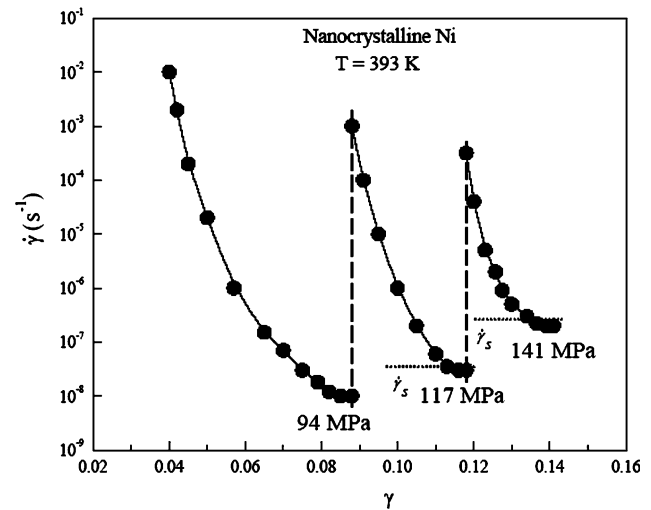


Fig. 2 A typical example for the results of stress increase tests performed on (ED) nc-Ni (initial grain size = 20 nm). Stress was increased from 94–117 to 141 MPa at 393 K; $\dot{\gamma}_s$ refers to the steady-state creep rate obtained during an uninterrupted test at corresponding stresses

surface free energy to lie in the plane of the specimen [24]. The figure also shows an extra peak of (300), which is not a standard reflection plane for FCC metals. This observation reveals the presence of a preferred texture with the {100} planes oriented predominantly in the as-electrodeposited samples.

Figure 3b shows a typical example for the XRD pattern for crept samples. As indicated by the figure, the extra peak of (300) is not present. In order to determine whether the conditions of creep testing (stress and temperature) are responsible for the disappearance of this peak, the XRD measurements were performed using the shoulder of the crept specimen, which was subjected to the same test temperature without stress. Figure 3c shows the extra peak does not exist in the XRD of the shoulder. This finding along with other similar findings related to just annealing specimens as shown by Fig. 3d indicates that the disappearance of the peak is due to heating the samples at test temperature.

Grain size and grain size distribution

In order to measure the average grain size and its distribution in (ED) nc-Ni, the technique of TEM was adopted. A number of representative TEM micrographs were obtained and analyzed to construct a histogram of distribution for as-received ED and deformed Ni samples. In constructing the histogram, about 200 grains were used to obtain a grain size distribution. In addition, the cross section of the nc-Ni

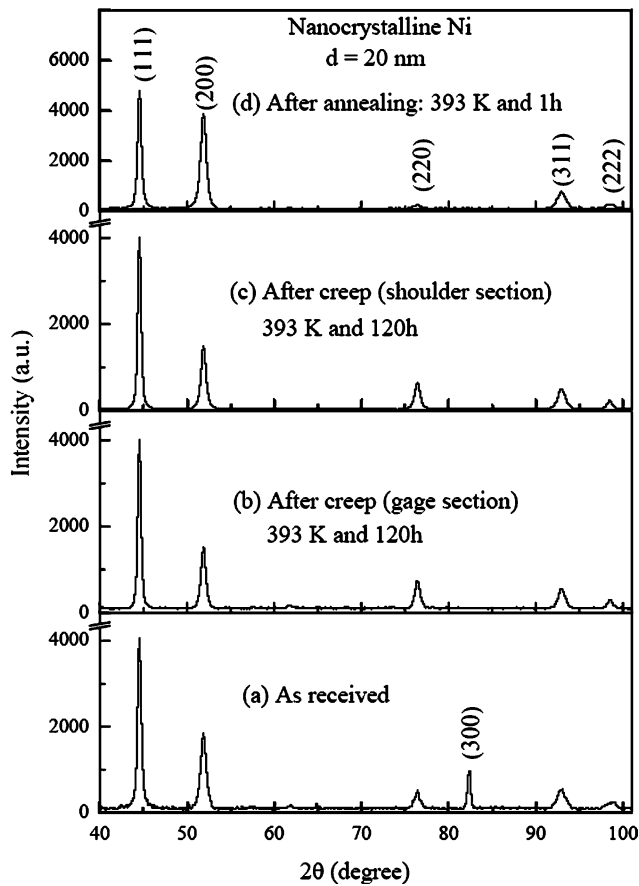


Fig. 3 XRD profiles for (ED) nc-Ni with an initial average grain size of 20 nm: (a) as-received, (b) the gage section of a sample after creep at 65 MPa and 393 K, (c) the shoulder section of the same sample after creep at 65 MPa and 393 K, and (d) the sample annealed at 393 K for 1 h

samples was examined for the purpose of determining whether columnar structures exist.

After carefully examining the representative TEM micrographs and histograms of the grain size distribution, the following results that characterize the initial microstructure and the microstructure after deformation are described herein:

1. Figure 4a, b shows a plan-view TEM micrograph and the grain size distribution plot, respectively, for the as-ED nc-Ni samples. From the histogram, the average grain size was estimated to about 24 nm.
2. An examination of the cross-section of the nc-Ni sheets (Fig. 5) shows the absence of columnar structures. Although the grains appear slightly longer than those seen in the plane view section of the sample, the average grain size in the cross-section view (25 nm) is close to that in the plane view section. According to available information (A. Robertson, Private communication, Integran

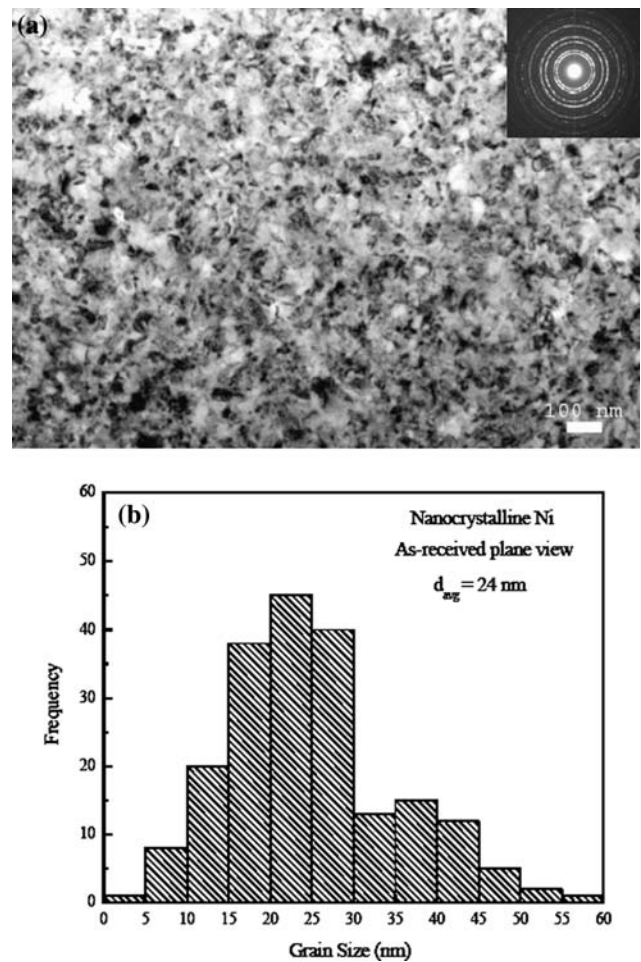


Fig. 4 (a) Bright field TEM micrograph showing the plane view of as-received (ED) nc-Ni, and (b) the grain size distribution of as-received (ED) nc-Ni

Technologies Inc.), the pulse waveforms used in the production of (ED) nc-Ni eliminates the risk of forming columnar growths that were observed in thick electrodeposits.

3. A TEM examination of nc-Ni samples that annealed for about 1 h (the total time to heat the sample to the test temperature and stabilize the temperature) showed that there was no significant grain growth; the average grain size is about 25 nm.
4. An examination of samples crept under the conditions of 393 K and 65 MPa showed that average grain size at the beginning of the steady-state stage was about 35 nm; and that during the steady state stage, the size did not significantly change (39 nm) (Figs. 6, 7), i.e., there was no significant grain growth once steady-state creep is reached (see Fig. 1). The samples were crept at 65 MPa for

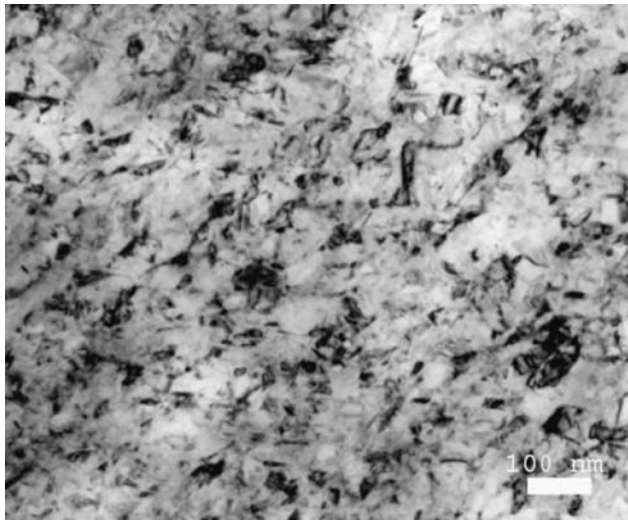


Fig. 5 Bright field TEM micrograph for the cross-section view of as-received (ED) nc-Ni, showing the absence of columnar structures

more than 5 days (>120 h). The maximum error in measuring the average grain size was ± 6 nm.

5. An examination of the sample shoulder (subjected to the test temperature without stress) indicated that the average grain size was about 27 nm after 5 days. This finding is consistent with the results of isothermal annealing (in the absence of applied stresses that have shown [23] the following trend: the rate of grain growth is very slow at 393 K as compared to that at 693 K.
6. An examination of samples crept at various stresses in the stress range used in the present investigation indicated that the average grain size was essentially the same and was equal to about 40 nm. For example, at 151 MPa, the average grain size was 37 nm (Table 2).

For the purpose of comparison, XRD was also used to determine the grain size of nc-Ni samples before and after deformation. The method of integral breadth (IB) [25] was adopted. Table 2 summarizes the average grain size values obtained before and after deformation in nc-Ni samples using XRD and TEM. The data of the table show that the average grain size values obtained by XRD are consistently lower than those obtained by TEM. This finding suggests that the use of XRD may lead to an underestimation of the average grain size.

Microstructural features after deformation

TEM investigation on nc-Ni samples was conducted after creep testing at 65 MPa and 393 K for 25 h (start

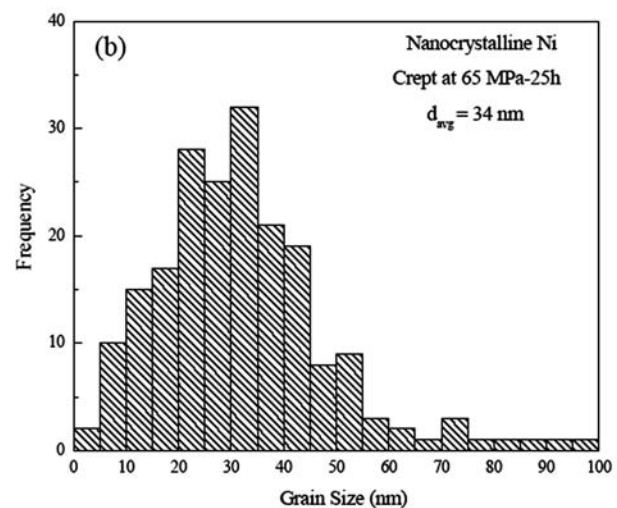
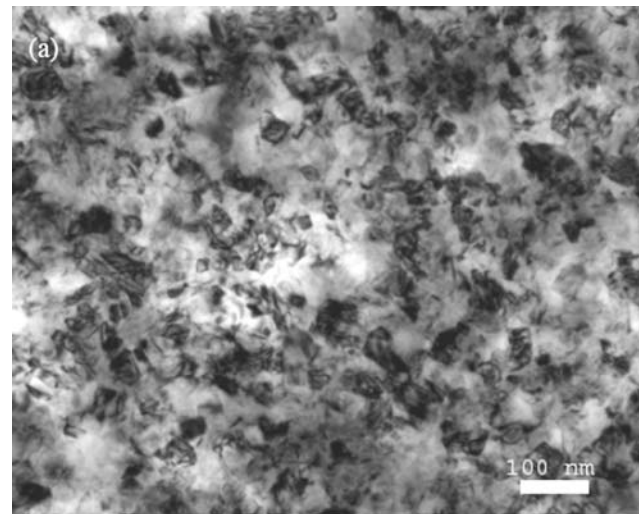


Fig. 6 (a) Bright field TEM micrograph and (b) the grain size distribution of (ED) nc-Ni crept at 393 K and 65 MPa for 25 h (start of steady state stage)

of steady state stage), and for more than 5 days (steady state stage). The microstructural features after deformation reveals following observations:

1. The microstructure consists of groups of grains (Fig. 8) with sharp grain boundaries. Curved grain boundaries are also noted in some of the grains. Most of the grains observed were equiaxed and free from dislocations.
2. Grain coalescence was also observed. As shown in Fig. 9, a group of grains with each grain having a size of about 10 nm coalesce together to form a big domain whose size is around 30 nm and larger.
3. Isolated dislocations are observed in only few grains (Fig. 10).

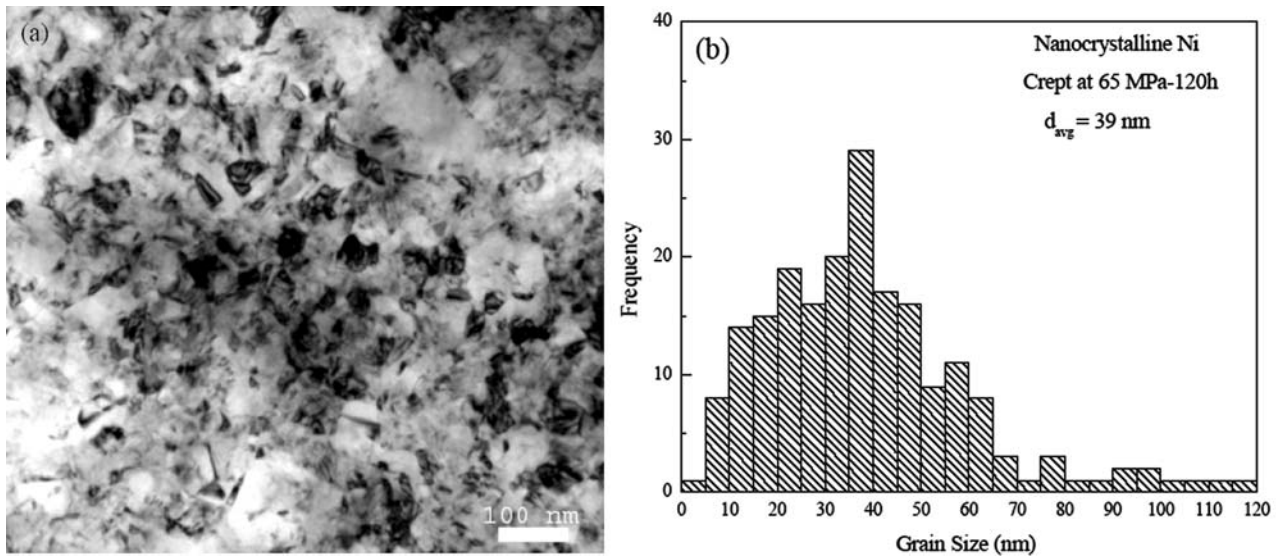


Fig. 7 (a) Bright field TEM micrograph and (b) the grain size distribution of (ED) nc-Ni crept at 393 K and 65 MPa to within steady state creep (>120 h)

Table 2 Comparison between the values of average grain size obtained from TEM and XRD

Conditions	Grain size (nm)	
	TEM	XRD
As ED	24 ± 6	20 ± 3
Annealed for 1 h	20 ± 6	21 ± 3
After creep 65 MPa, 25 h	34 ± 6	21 ± 3
After creep 65 MPa, 120 h	39 ± 6	22 ± 3

Discussion

Creep characteristics

According to the present results, the creep curve of (ED) nc-Ni obtained at three different stresses is characterized by the presence a well-defined steady-state stage. Also, the results show that the value of the steady-state strain rate is reproducible regardless of whether the creep rate is obtained from uninterrupted test or stress increase tests. These findings contrast with those recently reported for (ED) nc-Ni by Kottada and Chokshi [6], which indicated that the creep rate decreased continuously with time. Kottada and Chokshi [6] attributed this behavior to the occurrence of grain growth during creep. On the other hand, the present findings are in agreement with those of Yin et al. [5] who reported that for (ED) nc-Ni at 473 K, the creep curves exhibited minimum creep rates (equivalent to the steady-state creep rate).

When the applied stress is increased or decreased during a creep test, the stress exponent, *n*, can be estimated from the following expression:

$$n = \frac{\ln(\dot{\gamma}_1/\dot{\gamma}_2)}{\ln(\tau_1/\tau_2)} \tag{1}$$

Using the above expression, the values of *n* were estimated from the present creep tests are 5 and 10 for the stress increases from 94 to 117 MPa and from 117 to 141 MPa, respectively.

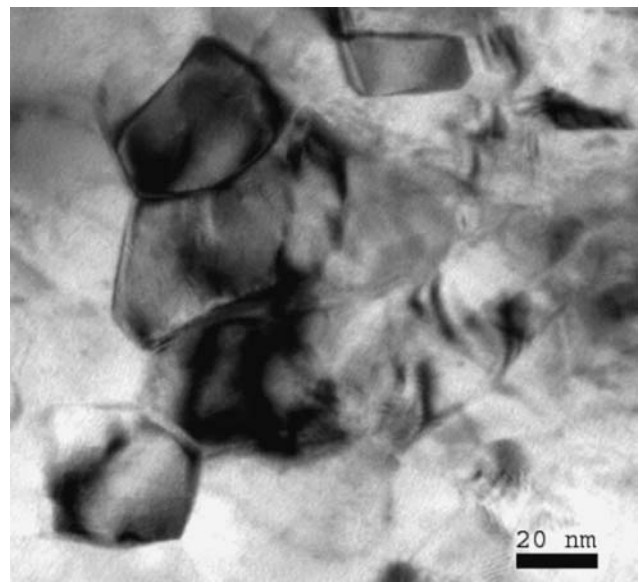


Fig. 8 TEM micrograph of (ED) nc-Ni sample crept at 393 K and 65 MPa showing the group of equiaxed grains

The present results on nc-Ni show that n for nc-Ni is high and variable. This trend cannot be explained by the Newtonian Coble process ($n = 1$) [26] even if it is assumed that the process is associated with a threshold stress, τ_0 , for initiating deformation; the presence of τ_0 would lead to an increase in the stress exponent with decreasing applied stress, a trend that contrasts with the experimental behavior. Also, triple junction creep [27], like Coble creep, is Newtonian in nature, and, therefore, cannot account for either the high values of the stress exponent or the variation in its value with applied stress.

Recently, Conrad and Narayan [28] have applied the concept of thermally activated processes to the description of the deformation behavior of nc-materials. The rate controlling equation is given by [28]:

$$\dot{\gamma} = \left(\frac{6bv_D}{d} \right) \exp \left(\frac{-\Delta F}{kT} \right) \sinh \left(\frac{\tau v}{kT} \right), \quad (2)$$

where b is the Burgers vector, v_D is the frequency of vibration, ΔF is the activation energy, k is Boltzmann's constant, T is the absolute temperature, v is the activation volume ($=b^3$) and τ is applied stress. According to Conrad and Narayan [28], the controlling process as a stress-assisted thermally activated motion in the grain boundary, in which the deformation rate is produced by independent atomic shear events (atomic jump processes). Under this condition, ΔF is equal to the activation energy for grain boundary diffusion. The apparent stress exponent is defined as:

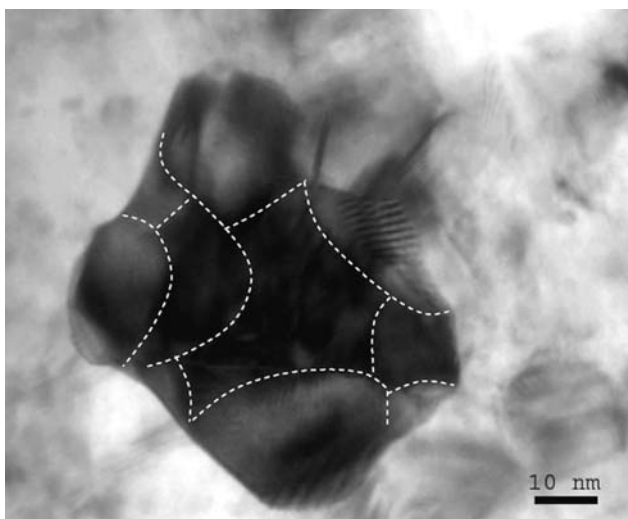


Fig. 9 (ED) nc-Ni samples crept at 393 K and 65 MPa showing bright field TEM micrograph of grain coalescence (marked by dotted lines)

$$n = \frac{\partial \ln(\dot{\gamma})}{\partial \ln(\tau)}. \quad (3)$$

By applying the above definition to Eq. 2, one obtains

$$n = \left(\frac{\tau v}{kT} \right) \coth \left(\frac{\tau v}{kT} \right). \quad (4)$$

Substituting $v = b^3$, $b = 0.249$ nm, $T = 393$ K and $k = 1.38 \times 10^{-23}$ J/K in Eq. 4 leads to a stress exponent of unity at all stresses applied; under the present conditions of stress and temperature, $\coth(\tau v/kT)$ reduces to $\tau v/kT$. Accordingly, the above deformation process as represented by Eq. 2 cannot account for the higher values of n that are measured in the present investigation.

Texture

While the exact reason for the observation of the extra peak of (300) in the XRD pattern for the as-received samples is not known (Fig. 3), two comments can be made. First, the disappearance of the peak upon

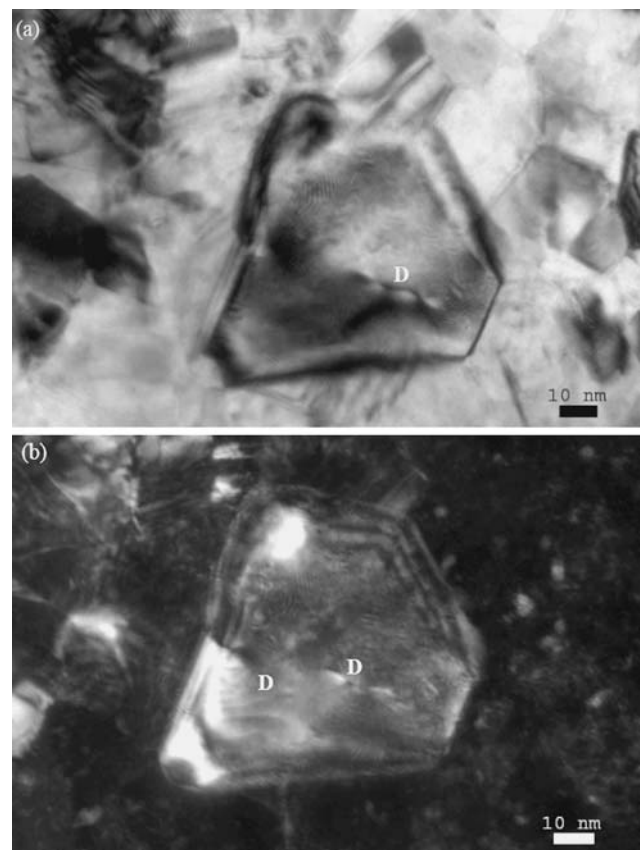


Fig. 10 (a) (ED) nc-Ni samples crept at 393 K and 65 MPa showing bright field TEM micrograph of isolated dislocations present in a grain (marked as *D*) and (b) dark field TEM micrograph of (a)

annealing ensures that this type of texture would not introduce any complications during the creep of nc-Ni samples. Second, according to very recent results dealing with thermal stability in (ED) nc-Ni [23], annealing the material at temperatures lower than $T < 450$ K has resulted in re-ordering boundaries without significant changes in the grain size. Since the texture related to the peak of (300) is not an equilibrium feature of the microstructure, its disappearance under favorable conditions such as thermal agitation resulting from annealing is expected.

Grain growth

Consideration of microstructural features after creep test illustrates that there is a stress induced grain growth in nc-Ni. Upon loading nc-Ni specimens at 393 K, grain growth continuously occurs. Once steady-state creep is attained, the grain growth ceases significantly (Fig. 1). The absence of significant grain growth is consistent with the presence of a well-defined steady state stage in the creep curve of nc-Ni (Fig. 1). If grain growth had been substantial, the creep rate would have exhibited a continuous decrease with time. Stress-induced grain growth was reported during creep [5], compression [6], high-pressure torsion [29] and nanoindentation of nc-materials [30]. Recently, in situ nanoindentation TEM reported [30, 31] that grain rotation and grain coalescence are two mechanisms responsible for the stress induced grain growth in nc-materials.

Detailed investigation to understand the stress induced grain growth is in progress. However, based on the microstructural evidences observed in the present study, a possible explanation may be offered. Upon loading, majority of small grains starts rotating and coalesce together, forming a large domain. The number of these coalesced domains, which eventually transform into large grains increases with time. When the number of the small grains that participate in rotation decreases below a critical value, significant grain growth ceases.

After performing stress increase tests, the steady-state creep rates obtained at the new stresses were essentially equal to those obtained in uninterrupted tests that were carried out at the new stresses (Fig. 2). This finding suggests that over the range of stresses used at 393 K, the grain size during steady-state creep is essentially the same. For example, if the grain size attained during steady-state creep at 94 MPa and 393 K (Fig. 2) had been different from that characterizing the steady-state creep rate measured in the uninterrupted test at 141 MPa, a stress increase from 94 to 141 MPa would not have led the observation

revealed by Fig. 2: the steady-state creep rate after the stress increase from 94 to 141 MPa is essentially equal to that obtained in the uninterrupted test at 141 MPa. As mentioned earlier, TEM observations showed that the average grain sizes measured after creep at various stresses in the range of stresses used essentially exhibited the same value of about 40 nm. This finding is consistent with the above suggestion.

The attainment of nearly the same grain size of about 40 nm over the range of stresses applied at 393 K suggests the presence of an upper limit for deformation induced grain growth under a certain combination of stress, temperature, and time. Very recent results by Liao et al. [29] appear to lend support to this suggestion. Those results have shown that during high-pressure torsion, there exists an upper limit for the deformation induced grain growth in nc-Ni, and that the final grain size will not change with further strain. Extrapolating those results leads to the possibility that the same upper limit of grain size during creep at the test temperature would be achieved under a certain combination of stress and time. This possibility is the subject of future research.

XRD was also used to investigate the stress induced grain growth in nc-Ni. After the completion of a creep test, XRD was conducted on the gage section of the sample to calculate the average grain size using IB method and compared with the values obtained from TEM (Table 2). Consideration of the results suggests that the average grain size value obtained from XRD for as-ED Ni sample was 20 ± 3 nm that agrees reasonably well with the TEM value (24 ± 6 nm). However, in the case of deformed samples, it appears that XRD underestimates the average grain size value. The values obtained from XRD for deformed samples were in the range of 20 to 22 nm, whereas the values estimated from TEM were in 35–40 nm range.

Conclusions

1. The creep curve obtained for (ED) nc-Ni is characterized by the presence of a well-defined steady-state stage.
2. Upon loading nc-Ni specimens at 393 K, grain growth occurs. However, once steady-state creep is reached, significant grain growth ceases.
3. The mechanism of grain growth appears to involve the rotation and the coalescence of small grains, forming a large domain that transforms into a large grain.
4. The present results suggest that after deformation, the average grain sizes measured by XRD are smaller than those obtained by means of TEM.

Acknowledgements This work was supported by National Science Foundation under Grant number DMR-0304629. Thanks are extended to Dr. Wen-An Chiou, Indranil Roy, and Li-Chung Lai for their assistance in some of the TEM work.

References

1. Gleiter H (1989) *Prog Mater Sci* 33:223
2. Gleiter H (2000) *Acta Mater* 48:1
3. Mohamed FA, Li Y (2001) *Mater Sci Eng A* 298A:1
4. Bird JE, Mukherjee AK, Dorn JE (1969) In: Brandon DG, Rosen A (eds) *Quantitative relation between properties and microstructures*. Israel University Press, Jerusalem, pp 255
5. Yin WM, Whang SH, Mirshams RA (2005) *Acta Mater* 53:383
6. Kottada RS, Chokshi AH (2005) *Scripta Mater* 53:887
7. Wang DL, Kong QP, Shui JP (1994) *Scripta Metall Mater* 31:47
8. Deng J, Wang DL, Kong QP, Shui JP (1995) *Scripta Metall Mater* 32:349
9. Xiao ML, Kong QP (1997) *Scripta Mater* 36:299
10. Wang N, Wang Z, Aust KT, Erb U (1997) *Mater Sci Eng A* 237A:150
11. Hahn H, Averback RS (1991) *J Am Ceram Soc* 74:2918
12. Yin WM, Whang SH, Mirshams RA, Xiao CH (2001) *Mater Sci Eng A* 301A:18
13. Dalla Torre F, Spätig P, Schäublin R, Victoria M (2005) *Acta Mater* 53:2337
14. Dalla Torre F, Van Swygenhoven H, Schäublin R, Spätig P, Victoria M (2005) *Scripta Mater* 53:23
15. Dalla Torre F, Van Swygenhoven H, Victoria M (2002) *Acta Mater* 50:3957
16. Kumar KS, Suresh S, Chisholm MF, Horton JA, Wang P (2003) *Acta Mater* 51:387
17. Wang YM, Chang S, Wei QM, Ma E, Nieh TG, Hamza A (2004) *Scripta Mater* 51:1023
18. Haasz TR, Aust KT, Palumbo G, El-Sherik AM, Erb U (1995) *Scripta Metall Mater* 32:423
19. Shei SA, Langdon TG (1978) *Acta Metall* 26:639
20. Yan S (1998) PhD Thesis. University of California, Irvine
21. Chirouze BY, Schwartz DM, Dorn JE (1967) *Trans Q AM Soc Metals* 60:51
22. Murty KL, Mohamed FA, Dorn JE (1972) *Acta Metall* 20:1009
23. Chauhan M, Mohamed FA (2006) *Mater Sci Eng A* 427:7
24. Mackenzie JK, Moore AJW, Nicholas JF (1962) *J Phys Chem Solids* 23:185
25. Kulig HP, Alexander LE (1974) Wiley, New York, pp 661
26. Coble RL (1963) *J Appl Phys* 34:1679
27. Wang N, Wang Z, Aust KT, Erb U (1995) *Acta Metall Mater* 43:519
28. Conrad H, Narayan J (2000) *Scripta Mater* 42:1025
29. Liao XZ, Kilmametov AR, Valiev RZ, Gao H, Li X, Mukherjee AK, Bingert JF, Zhu YT (2006) *Appl Phys Lett* 88:021909
30. Shan ZW, Stach EA, Wieszorek JMK, Knapp JA, Follstaedt DM, Mao SX (2004) *Science* 305:654
31. Jin M, Minor AM, Stach EA, Morris JW (2004) *Acta Mater* 52:5381